An Analysis of How Driver Experience Affects Eye-Gaze Behavior for Robotic Wheelchair Operation

Yamato Maekawa, Naoki Akai, Takatsugu Hirayama, Luis Yoichi Morales,
Daisuke Deguchi, Yasutomo Kawanishi, Ichiro Ide, Hiroshi Murase
Nagoya University, Japan

maekaway@murase.is.i.nagoya-u.ac.jp, morales_yoichi@coi.nagoya-u.ac.jp,
{akai, takatsugu.hirayama, ddeguchi}@nagoya-u.jp, {kawanishi,ide,murase}@i.nagoya-u.ac.jp

Abstract

Drivers obtain information on surrounding environment using their eyesights. Experienced eye-gaze behavior is needed when driving at places where multiple risks exist to prepare for and avoid them. In this work, we analyze the change in eye-gaze behavior in such situations while a driver gains experience on the operation of a robotic wheelchair. Accurate distance information in the traffic environment is important to analyze the eye-gaze behavior. However, almost all previous works analyze eye-gaze behavior in a 2D environment, so they could not obtain accurate distance information. For this reason, we analyze eye-gaze behavior in 3D space. Concretely, we developed a novel eye-gaze behavior analysis platform based on a robotic wheelchair and estimated the driver's attention in 3D space. We try to analyze the eye-gaze behavior considering a useful field-of-view in 3D space based on the distance information instead of only the fixation point to investigate the objects that a driver implicitly pays attention to and from where s/he focuses on them. Results show that novice drivers pay attention to a single risk at a time. In contrast, they pay more attention to multiple risks simultaneously as they gain experience. Additionally, we discuss what features are effective to model the eye-gaze behavior based on the results.

1. Introduction

The demand for personal mobility vehicles like an electric wheelchair is increasing. However, while people can move easily driving them, they can also cause many traffic accidents. In general, drivers obtain information on surrounding environment using their eyesights, but several studies report that the eye-gaze behavior of expert drivers differ from that of novice drivers [23]. However, the difference in eye-gaze behavior between expert and novice

(a) Driver's view with gaze point.

(b) Eye-tracking glasses.

(c) Visualization on the 3D map

(d) Robotic wheelchair.
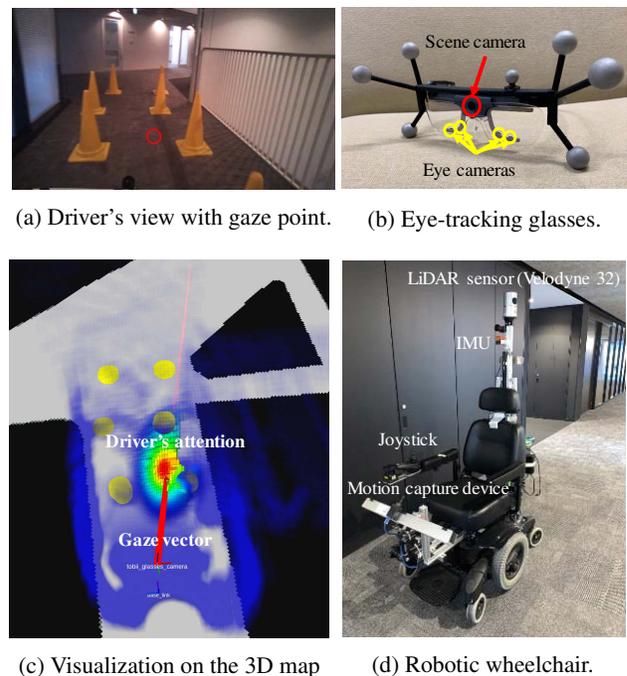
Figure 1: Concept of the analysis. We use a robotic wheelchair (d) equipped with sensors and eye-tracking glasses (b). (c) shows an example of a visualization of the driver's gaze vector and attention on the 3D map. The gray area and the yellow circles represent the course and the obstacles respectively.

drivers have not been clarified at places with multiple risks where experience plays a huge role.

Our motivation is to investigate the objects that a driver implicitly pays attention to and from where s/he focuses on them. This requires analyzing eye-gaze behavior in 3D space. Since almost all past works analyze eye-gaze behavior in 2D environment [4, 15], the analyses were limited

due to the difficulty of obtaining accurate distance information. Additionally, most previous studies [17, 20] analyze the eye-gaze behavior based on the fixation point. However, they could only determine what drivers strongly focus on although they are actually implicitly paying attention in a wider range of field-of-view. To overcome these problems, we consider the useful field-of-view in 3D space which spreads like an elliptical cone from the driver's eyes based on the distance information instead of only the fixation point.

For analyzing the eye-gaze behavior in 3D space, we developed a novel eye-gaze behavior analysis platform as shown in Figure 1. The platform is implemented on a robotic wheelchair (d) and it can recognize its own accurate pose on a 3D map (c). Additionally, the wheelchair is equipped with a motion capture device in its front to track eye-tracking glasses with motion capture markers which estimates their poses. Based on pose estimation of the wheelchair and eye-tracking glasses with eye-gaze measurement results, we can estimate the driver's eye-gaze vector in the 3D map. As a result, we can analyze the eye-gaze behavior taking accurate distance information into consideration.

To prevent traffic accidents in a place with multiple risks, we consider that it would be effective to support visual cognition of drivers by presenting as a reference, the eye-gaze behavior of experienced drivers. For this, in this work, to model the eye-gaze behavior of experienced drivers, we analyze the change in eye-gaze behavior when a driver gains experience on the operation of the robotic wheelchair. We prepared a narrow course with blind corners as the place with multiple risks, which we assume that experienced drivers can pay attention to all of them at the same time. To confirm this assumption, we establish hypotheses for eye-gaze behavior to clarify the difference between experienced and novice drivers. Results from an experiment using the robotic wheelchair show that novice drivers pay their attention to a single risk at a time, but eventually they pay more attention to multiple risks as they gain experience. Finally, we will discuss what features are effective to model the eye-gaze behavior based on the results.

The contributions of this paper are as follows:

- We develop a 3D measurement technology to estimate what a driver focuses on considering the useful field-of-view as an elliptical cone.

- We analyze how driver experience affects eye-gaze behavior for robotic wheelchair operation in a narrow course with blind corners where multiple risks exist and discuss how to model them.

The rest of this paper is organized as follows. Section 2 summarizes related work. Section 3 describes our analysis methodology of eye-gaze behavior in 3D space. Section 4 describes the metrics for analyzing the eye-gaze behavior. Section 5 details an experiment in which inexperienced participants drive the robotic wheelchair. Section 6 reports the analysis of the relationship between driving experience and eye-gaze behavior. Finally, we conclude with a brief summary in Section 7.

2. Related work

In general, regardless to the task, eye-gaze behavior is different between experienced and novice persons. The difference is mainly due to experience and knowledge. For example, Iwatsuki *et al*. [7] analyzed that an experienced soccer coach gazes at the ball at high frequency when it is located in the middle of the soccer field, and at low frequency when it is located in front of either goal, whereas a novice coach gazes to the ball at high frequency regardless of where it is located. Such differences are studied in various fields, *e.g*., chess [18], bonsai [14], and other sports [7, 11, 25].

Such a difference is also seen in driving scenarios. Several studies report that eye-gaze behavior differs between experienced and novice drivers. Underwood *et al*. [23] analyzed that scanpaths in eye movements differ. They analyzed the scanpath between subdivided regions of a driving scene such as near left, far ahead, and mid right on the road. On the other hand, the aim of our work is the detailed analysis of what drivers look and from where drivers pay attention to. Van Leeuwen *et al*. [24] found that horizontal gaze variance decreases and the percentage of gazing at the center of the road increases as drivers gain driving experience. However, what the drivers look at was not clarified in their study. Pradhan *et al*. [16] report that risk perception of experienced drivers is higher than that of novice drivers in many situations. In addition, these works [16, 24] are performed on driving simulators which is limited to 2D visual environments. In our work, we analyze what the driver looks at in a situation with multiple risks when driving in an actual environment.

3. Analysis methodology of eye-gaze behavior in 3D space

In this section, we describe how to analyze the eye-gaze behavior in 3D space. The experimental robotic wheelchair we developed for acquiring driving data is shown in Figure 1(d). A LiDAR sensor[1], Inertial Measurement Unit (IMU)[2], and motion capture device[3] are attached to it. Tobii Pro Glasses 2 is used as eye-tracking glasses to acquire eye-gaze behavior data, as shown in Figure 1(b). We can estimate the position and orientation of eye-tracking glasses by

---

[1]Velodyne HDL-32
[2]Xsens MTi-300-2A5G4
[3]Optitrack V120:TRIO
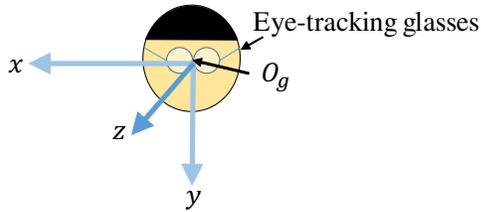
Figure 2: Coordinate system of the eye-tracking glasses.

Figure 3: Human field-of-view.

attaching spherical markers to the eye-tracking glasses and tracking them with the motion capture device.

3.1. Localization

To analyze in 3D space, we need to localize the robotic wheelchair on a 3D map. We make a 3D map with Simultaneous Localization and Mapping (SLAM) [5] using LiDAR beforehand. Then, we estimate the position of the robotic wheelchair on the map with Adaptive Monte Carlo Localization (AMCL) [2, 22] using the 3D point cloud acquired from the LiDAR, the 3D map and odometry information estimated from velocity, acceleration, and angular velocity of the robotic wheelchair. We define the coordinate system of the robotic wheelchair in the map. We also define the coordinate systems of the LiDAR sensor and the motion capture device by measuring relative positions and orientations from the coordinate system of the robotic wheelchair. Based on them, we estimate their positions and orientations on the 3D map. Furthermore, the position and orientation of eye-tracking glasses with spherical markers on the 3D map are estimated from the tracking results of the motion capture device. Based on the results and eye-gaze measurement, we estimate the gaze vector in the 3D map. As shown in Figure 2, we take x, y, and z-axes whose origin (O_g) is the position of the scene camera of the eye-tracking glasses as shown in Figure 1(b).

3.2. Determining objects in the useful field-of-view

We consider the field-of-view to analyze eye-gaze behavior. It is roughly divided into the central and peripheral visual fields, as shown in Figure 3. The closer an area is to the gaze point, the clearer it is visually. The region where an object is relatively clearly visible in the peripheral visual field is called the useful field-of-view. Almost all previous studies determine an object in the central visual field as the focused object. However, it is not an appropriate determination because drivers do not necessarily look at an object only in their central visual field, but they also pay attention to objects in the useful field-of-view, too [13]. For this reason, we determine the focused object considering the useful field-of-view. We need to analyze in 3D space because the useful field-of-view spreads like an elliptical cone from the driver's eyes.
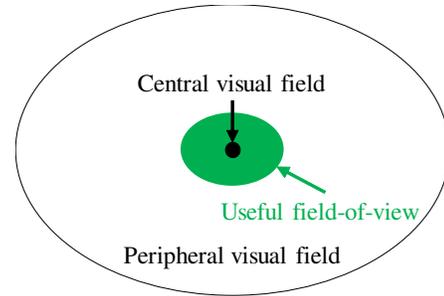
We determine objects in the useful field-of-view by using the gaze vector and 3D point cloud. An object is determined to be in the useful field-of-view if its 3D point cloud exists within the field, as shown in Figure 4(a). The useful field-of-view differs according to psychological factors, age, and so on. In this paper, we define the range of the useful field-of-view as between 15 degrees on both left and right sides, and 8 degrees above and 12 degrees below according to Hatada's definition [6].

First, we draw a line connecting O_g and point p in a 3D point cloud, and then determine the intersection point of the line and the x-y plane ($z = 1$) as shown in Figure 4(b). Similarly, we determine the intersection point of the gaze vector and the x-y plane ($z = 1$). Then, we determine angle α between the line connecting these intersections and the x-axis. The elliptical circumference in Figure 4(c) shows the useful field-of-view. The line segments shown in Figures 4(b) and 4(c) are the same. As shown in Figure 4(c), the boundary angle corresponding to angle α is determined. Finally, we determine angle β of the line connecting O_g and p and the gaze vector as shown in Figure 4(a), and compare β with the boundary angle. If β is smaller than the boundary angle, the object is assumed to be in the useful field-of-view. This process is applied to each point in the 3D point cloud.

4. Hypotheses and metrics for the analysis

This section describes the hypotheses on the eye-gaze behavior on a narrow course with blind corners to clarify the difference between experienced and novice drivers. To confirm these hypotheses, metrics for analyzing eye-gaze behavior are proposed.

4.1. Hypotheses for eye-gaze behavior on a narrow course with blind corners

We consider a narrow course with blind corners on both sides. The risks here are represented mostly by the following two.

- Robotic wheelchair deviating from the drivable path.
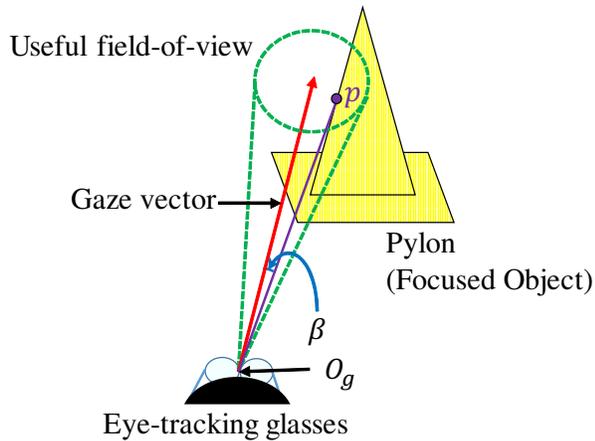
(a) Focused object in the useful field-of-view, *e.g.*, pylon. The purple line represents the line connecting the origin O_g and point p in a 3D point cloud.

(b) Projection onto the x-y plane ($z = 1$).

(c) Boundary.
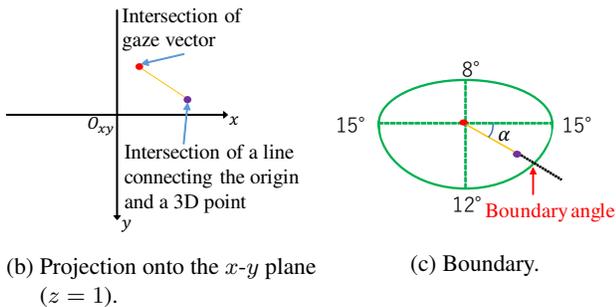
Figure 4: Determination of focused objects in the useful field-of-view.

- Pedestrian suddenly running out in front of the robotic wheelchair.

Based on the above, we establish hypotheses for the change in eye-gaze behavior in relation to the increase of robotic wheelchair driving experience as follows:

- Eye-gaze behavior of a novice driver is mostly focused on not deviating from the drivable path.

- Eye-gaze behavior of an experienced driver is balanced between averting both risks mentioned above.

4.2. Metrics for analyzing eye-gaze behavior

We assume that analyzing to what, from where, and how drivers pay their attention is important when analyzing the change in eye-gaze behavior in relation to the increase of driving experience. We propose the following metrics on gaze direction and the focused object.

- Gaze direction metric
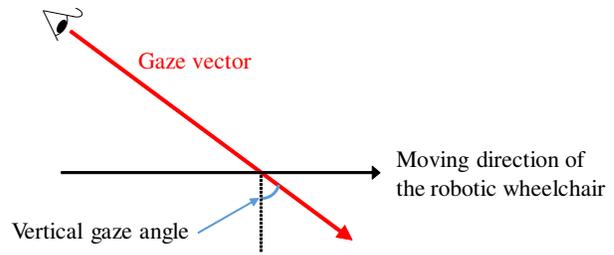
Figure 5: Definition of vertical gaze angle.

　　– Vertical gaze angle
- Focused object metrics
　　– Gaze frequency
　　– Proportion of focusing time
　　– Distance to the focused object

4.2.1 Gaze direction metric

We assume that novice drivers tend to look downwards to recognize the running path. In contrast, we assume that experienced drivers tend to look ahead because they are careful with pedestrians suddenly running out from the blind corners and recognize the drivable path further away. To confirm these assumptions, we set vertical gaze angle as the gaze direction metric. Figure 5 shows the vertical gaze angle when the robotic wheelchair is viewed from the side. First, we transform the gaze vector from the eye-tracking glasses coordinates to the robotic wheelchair coordinates. Here, we define the pitch on the robotic wheelchair coordinate system as the vertical gaze angle. Note that it takes 0 degrees when the driver looks vertically down and 180 degrees when the driver looks vertically up.

4.2.2 Focused object metrics

We also use gaze frequency, the proportion of focusing time, and the distance to the focused object as the focused object metrics. The gaze frequency represents the number of times a driver pays attention to a specific object within a specific period. The proportion of focusing time is the total time an object is focused on divided by the total length of the data. These have been used in previous studies [3]. We assume that the gaze frequency and the proportion of focusing time to the blind corners by experienced drivers are higher compared to novice drivers. Here, we propose the distance to the focused object in addition to these two metrics. It represents the distance of a driver to the object s/he is focusing on. We assume that experienced drivers move their eyes to detect and prepare for risks earlier than novice drivers.

5. Experiment

We conducted an experiment where inexperienced participants drove the robotic wheelchair to confirm our hypotheses described in Section 4. Here, we define participants without driving experience as novice drivers and participants with driving experience as experienced drivers. In other words, the experiment participants will transit from novice to experienced drivers during the experiment. We analyze the change in eye-gaze behavior as drivers gain experience. In this section, we describe the actual experiment course, the experiment procedure, and the acquired data.

5.1. Experiment course

We conducted the experiment in an indoor environment at our University. Figure 6(a) shows the map of the indoor environment. A narrow course was simulated by placing pylons on a corridor. We analyzed the data acquired in the green area shown in Figure 6(b). Figure 6(c) shows the layout of the pylons. As shown in Figure 6(b), there are blind corners on both sides.

5.2. Experiment procedure

First, we instructed the experiment participants as follows:

- There are some people on this floor and some of them may run out. Be careful of pedestrians.

- There is a section where pylons are placed on the route. Pass between the pylons there.

- Do not collide with the pylons.

Then, the participants practiced driving the wheelchair on the above course for three laps. The pylons were not set at this time. After the practice, we set the pylons and instructed the participants to drive 29 laps There was a 30-second break between laps and the participants could take an additional break if they got tired. An experiment collaborator ran out in front of the robotic wheelchair from each blind corner in order to make the participants aware of risks. The events took place twice from each blind corner and on laps 6, 12, 18, and 24. Note that we do not use data including the events or acquired on laps where a collision with a pylon accidentally occurred.

We measured the eye-gaze behaviors of five participants; male students in their twenties and are inexperienced with driving robotic wheelchairs before participating. Note that this experiment was conducted after obtaining the approval of the Ethics Committee of the University.

5.3. Acquired data

We acquired the following data through the experiment.
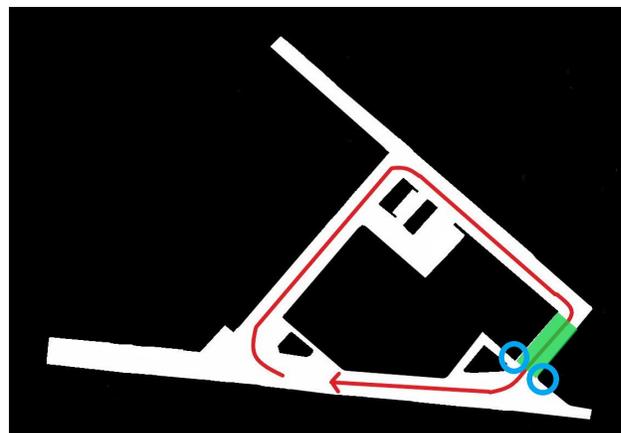
(a) Floor map. Experiment participants drove along the red line in clockwise.

(b) Experiment course.
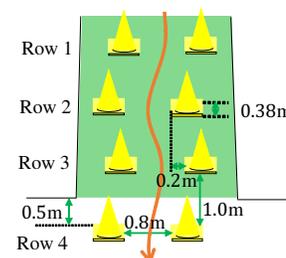
(c) Layout of pylons. The robotic wheelchair cannot keep running straight when passing between pylons.

Figure 6: Experiment course and layout of pylons. We acquired data in the green area. Blue circles indicate blind corners. While there were unrelated people walking in the vicinity, only the experiment participants and collaborators entered the green area.

- Image from scene camera embedded on eye-tracking glasses (25 Hz)

- Gaze vector (25 Hz)

- 3D point cloud of the surrounding environment from the LiDAR (10 Hz)

- Velocity and acceleration of the robotic wheelchair (30 Hz)

- Acceleration and angular velocity from IMU (80 Hz)

- Position and orientation of eye-tracking glasses from motion capture device (125 Hz)
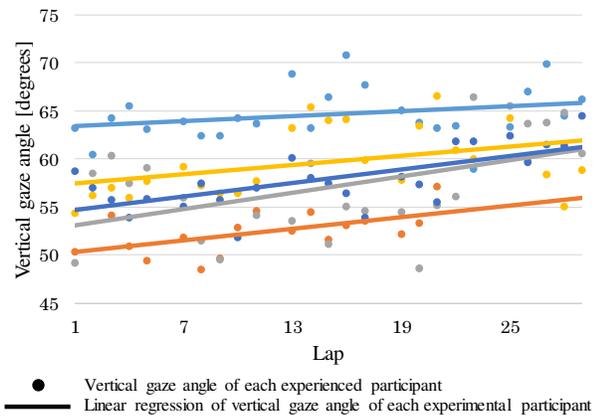
Figure 7: Vertical gaze angle of each experiment.

Note that we synchronized the data based on the timestamp of the gaze vector.

6. Analysis of the relationship between driving experience and eye-gaze behavior

We analyze the obtained eye-gaze behavior based on the metrics described in Section 4.

6.1. Analysis by gaze direction metric

Figure 7 shows the vertical gaze angles of each experiment participant on each lap and their linear regression calculated by the least-squares method. The linear regression lines of all participants show an upward trend. This is because they looked at nearby pylons to prevent the wheelchair from colliding with them while they were inexperience. However, they eventually looked at pylons further away and became aware that pedestrians might suddenly run out from the blind corners as they gained driving experience.

6.2. Analysis by focused object metrics

Next, we analyze what and from where the experiment participants focused on using the focused object metrics. The objects are classified into "pylons", "blind corners", and "others". Additionally, the pylons are divided into the first, the second, the third, and the fourth row pylons in order of passage as shown in Figure 6(c). Although the pylons and the blind corners exist on both sides, we do not distinguish them to calculate the gaze frequency and the proportion of focusing time. We divide the data per five laps into laps 1–5, laps 7–11, laps 13–17, laps 19–23, and laps 25–29. Figure 8 shows the average gaze frequency and the proportion of focusing time for the blind corners for five participants. The proportion of focusing time to the blind corners
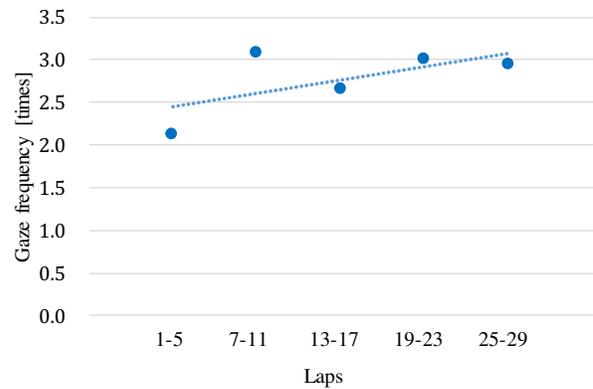
(a) Gaze frequency.
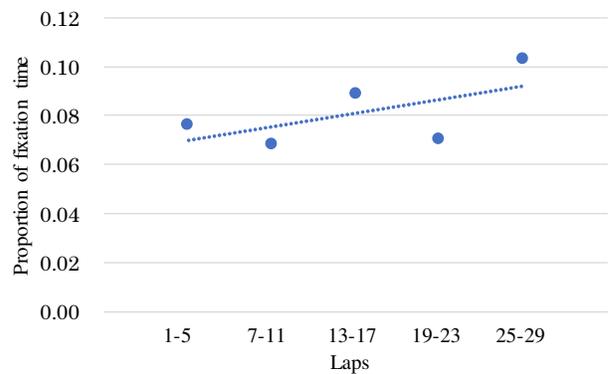
(b) Proportion of focusing time.

Figure 8: Gaze frequency and proportion of focusing time to the blind corners. Dotted lines represent the linear regression calculated by the least squares method. Note that we do not analyze data on laps 6, 12, 18, and 24 because an experiment collaborator ran out in front of the robotic wheelchair from each blind corner.

increases, meaning the participants increased the duration they paid attention to the blind corners so they could prepare for pedestrians running out as they gained driving experience.

We analyze from where the participants focused on the pylons referring to the distance to the focused objects. The distance from the blind corners are defined as shown in Figure 9. The distance is discretized at an interval of 0.1 m and the proportion of focusing time to each pylon is calculated at each interval, as shown in Figure 10. Note that the robotic wheelchair ran from left to right in the figure. As a result, the proportion of focusing time to each pylon from a distant position increased as drivers gained driving experience. This is because the participants' eye-gaze be-
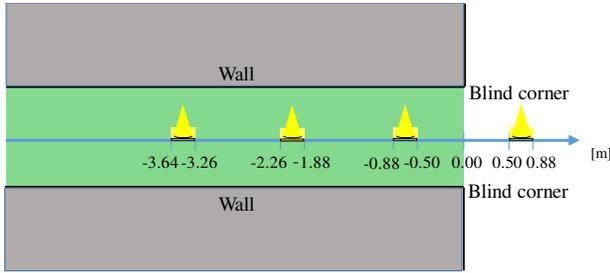
Figure 9: Distance of pylons from the blind corners.

haviors changed to capture distant pylons, i.e. the third and the fourth row of pylons, in the useful field-of-view while keeping their attention to nearby pylons to prevent the wheelchair from colliding with them. Moreover, the timing to remove each pylon from the useful field-of-view became earlier as they gained driving experience. This is because they switched their gaze earlier to prepare for other risks.

Summarizing the obtained results, we can confirm that the novice drivers looked at nearby pylons to prevent the robotic wheelchair from colliding with them, but as they gained driving experience, they started paying attention to multiple risks by focusing on further pylons and allocating more time to focus on blind corners.

6.3. Discussion

Our final objective is to model the eye-gaze behavior of expert and novice drivers separately since we need to understand the causes behind the difference in the eye-gaze behaviors. There are various behavior modeling methods [12, 15] and inverse reinforcement learning (IRL) [9, 10, 19, 21] is widely used recently. In IRL, features that might significantly influence the behaviors are extracted [10, 21]. It is better to prepare a set of appropriate features before applying IRL. The analysis in this paper can be considered as an exploration of features in IRL.

Through the experiments, we confirmed that the metrics changed as drivers gained driving experience. We consider that these metrics are useful as the features that represent the difference of expert and novice drivers to model the eye-gaze behavior. For example, the proportion of focusing time to blind corners increased as shown in Figure 8(b). It indicates that while the novice drivers looked mostly at the pylons, they paid much attention to blind corners as they gained driving experience. If we can model these behaviors, we consider that the model of novice drivers weights the feature of pylons mostly, while that of expert drivers weights the feature of pylons and blind corners in a good balance referring to the proportion of focusing time on pylons and blind corners as features.
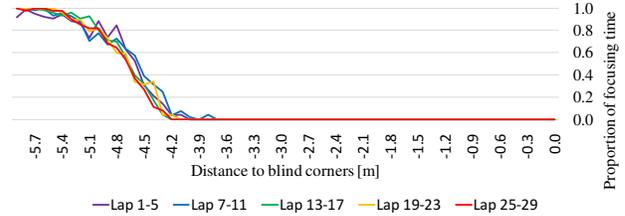
(a) The first row pylon.
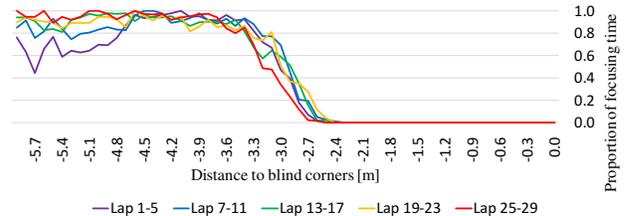
(b) The second row pylon.
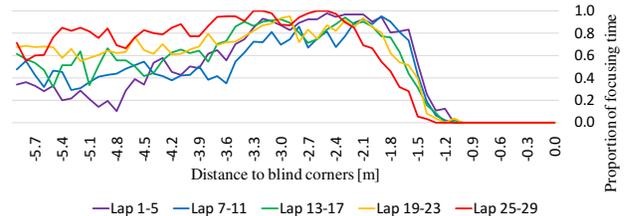
(c) The third row pylon.
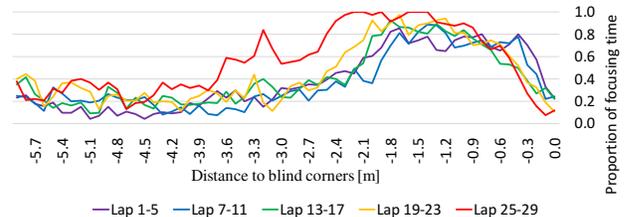
(d) The fourth row pylon.

Figure 10: Proportion of focusing time to the pylons.

7. Conclusion

We analyzed how driver experience affects eye-gaze behavior for robotic wheelchair operation, as an initial study for modeling the eye-gaze behavior of experienced drivers. First, we established hypotheses for eye-gaze behavior on a narrow course with blind corners and proposed metrics for analyzing eye-gaze behaviors in 3D space. Then, we conducted a driving experiment using a robotic wheelchair, in which the participants were inexperienced drivers. As a result, we confirmed our hypotheses:

- A novice driver's eye-gaze behavior is to stay on the drivable path.

- An experienced driver's eye-gaze behavior is well balanced between staying on the drivable path and taking caution to pedestrians suddenly running out.

Future works will include an extension of the dataset, comparison of results between previous 2D and our 3D analysis methodologies, and analysis in various situations and environments. We also plan to apply IRL [9, 19, 21] and Autoregressive Input-Output HMM (AIOHMM) [1, 8] to model eye-gaze behavior of experienced robotic wheelchair drivers.

Acknowledgements

References

[1] Naoki Akai, Takatsugu Hirayama, Luis Y. Morales, Yasuhiro Akagi, Hailong Liu, and Hiroshi Murase. Driving behavior modeling based on hidden Markov models with driver's eye-gaze measurement and ego-vehicle localization. *Proceedings of the 2019 IEEE Intelligent Vehicles Symposium*, pages 828–835, 2019.

[2] Naoki Akai, Luis Y. Morales, and Hiroshi Murase. Mobile robot localization considering class of sensor observations. *Proceedings of the 2018 IEEE/RSJ Conference on Intelligent Robots and Systems*, pages 3159–3166, 2018.

[3] Peta Baxter, Chiara De Jong, Rian Aarts, Mirjam de Haas, and Paul Vogt. The effect of age on engagement in preschoolers' child-robot interactions. *Proceedings of the Companion of the 2017 ACM/IEEE International Conference on Human-Robot Interaction*, pages 81–82, 2017.

[4] Roland Bremond, Jean Michel Auberlet, Viola Cavallo, Lara Désiré, Vérane Faure, Sophie Lemonnier, Régis Lobjois, and Jean Philippe Tarel. Where we look when we drive: A multidisciplinary approach. *Proceedings of the TRA — Transport Research Arena*, 10 pages, 2014.

[5] Giorgio Grisetti, Cyrill Stachniss, and Wolfram Burgard. Improved techniques for grid mapping with Rao-Blackwellized particle filters. *IEEE Transactions on Robotics*, 23(1):34–46, 2007.

[6] Toyohiko Hatada. Psychological and physiological analysis of stereoscopic vision. *Journal of Robotics and Mechatronics*, 4(1):13–19, 1992.

[7] Atsushi Iwatsuki, Takatsugu Hirayama, and Kenji Mase. Analysis of soccer coach's eye gaze behavior. *Proceedings of the 2nd IAPR Asian Conference on Pattern Recognition*, pages 793–797, 2013.

[8] Ashesh Jain, Hema S. Koppula, Bharad Raghavan, Shane Soh, and Ashutosh Saxena. Car that knows before you do: Anticipating maneuvers via learning temporal driving models. *Proceedings of the 15th IEEE International Conference on Computer Vision*, pages 3182–3190, 2015.

[9] Kris M. Kitani, Brian D. Ziebart, James A. Bagnell, and Martial Hebert. Activity forecasting. *Proceedings of the 12th European conference on Computer Vision*, pages 201–214, 2012.

[10] Markus Kuderer, Shilpa Gulati, and Wolfram Burgard. Learning driving styles for autonomous vehicles from demonstration. *Proceedings of the 2015 IEEE International Conference on Robotics and Automation*, pages 2641–2646, 2015.

[11] Derek T.Y. Mann, A. Mark Williams, Paul Ward, and Christopher M. Janelle. Perceptual-cognitive expertise in sport: A meta-analysis. *Journal of Sport and Exercise Psychology*, 29(4):457–478, 2007.

[12] Sujitha Martin, Sourabh Vora, Kevan Yuen, and Mohan M. Trivedi. Dynamics of driver's gaze: Explorations in behavior modeling and maneuver prediction. *IEEE Transactions on Intelligent Vehicles*, 3(2):141–150, 2018.

[13] Toshiaki Miura. Visual search in intersections: An underlying mechanism. *IATSS Research*, 16:42–49, 1992.

[14] Toshiaki Miura. Eye movements in appreciation of bonsais: The effect of knowledge and experience. *Proceedings of the 16th Congress of International Association of Empirical Aesthetics*, pages 95–96, 2000.

[15] Andrea Palazzi, Davide Abati, Simone Calderara, Francesco Solera, and Rita Cucchiara. Predicting the driver's focus of attention: The dr(eye)ve project. *IEEE Transactions on Pattern Analysis and Machine Intelligence*, 41(7):1720–1733, 2018.

[16] Anuj Pradhan, Kim R Hammel, Rosa Deramus, Alexander Pollatsek, David Noyce, and Donald Fisher. Using eye movements to evaluate effects of driver age on risk perception in a driving simulator. *Human Factors*, 47(4):840–52, 2005.

[17] Umesh Rajashekar, Lawrence K. Cormack, and Alan C. Bovik. Point-of-gaze analysis reveals visual search strategies. *Proceedings of the SPIE Human Vision and Electronic Imaging IX*, 5292:296–306, 2004.

[18] Eyal M. Reingold, Neil Charness, Marc Pomplun, and Dave M. Stampe. Visual span in expert chess players: evidence from eye movements. *Psychological Science*, 12(1):48–55, 2001.

[19] Nicholas Rhinehart and Kris M. Kitani. First-person activity forecasting with online inverse reinforcement learning. *Proceeding of the 16th IEEE International Conference on Computer Vision*, pages 3696–3705, 2017.

[20] Julian Schwehr and Volker Willert. Multi-hypothesis multi-model driver's gaze target tracking. *Proceedings of the 21st International Conference on Intelligent Transportation Systems*, pages 1427–1434, 2018.

[21] Masamichi Shimosaka, Takuhiro Kaneko, and Kentaro Nishi. Modeling risk anticipation and defensive driving on residential roads with inverse reinforcement learning. *Proceedings of the 17th International IEEE Conference on Intelligent Transportation Systems*, pages 1694–1700, 2014.

[22] Sebastian Thrun, Dieter Fox, Wolfram Burgard, and Frank Dellaert. Monte Carlo localization for mobile robots. *Proceedings of the 1999 IEEE International Conference on Robotics and Automation*, pages 1322–1328, 1999.

[23] Geoffrey Underwood, Peter Chapman, Neil Brocklehurst, Jean Underwood, and David Crundall. Visual attention while driving: Sequences of eye fixations made by experienced and novice drivers. *Ergonomics*, 46(6):629–649, 2003.

[24] Peter M. van Leeuwen, Riender Happee, and Joost C.F. de Winter. Changes of driving performance and gaze behavior of novice drivers during a 30-min simulator-based training. *Procedia Manufacturing*, 3:3325–3332, 2015.

[25] A. Mark Williams, Keith Davids, Les Burwitz, and John G. Williams. Visual search strategies in experienced and inexperienced soccer players. *Research Quarterly for Exercise and Sport*, 65(2):127–135, 1994.